Published in final edited form as:
Brain Struct Funct. 2010 May ; 214(4): 361–373. doi:10.1007/s00429-009-0238-0.

Quantification of the spatiotemporal microstructural organization of the human brain association, projection and commissural pathways across the lifespan using diffusion tensor tractography

Khader M. Hasan, **Arash Kamali**, **Humaira Abid**, **Larry A. Kramer**, **Jack M. Fletcher**, and **Linda Ewing-Cobbs**

K. M. Hasan · A. Kamali · H. Abid · L. A. Kramer, Department of Diagnostic and Interventional Imaging, University of Texas Medical School at Houston-Medical School, 6431 Fannin Street, MSB 2.100, Houston, TX 77030, USA, Khader.M.Hasan@uth.tmc.edu

L. Ewing-Cobbs, Department of Pediatrics, University of Texas Health Science Center at Houston-Medical School, Houston, TX, USA

J. M. Fletcher, Psychology Department, University of Houston, Houston, TX, USA

Abstract

Using diffusion tensor tractography, we quantified the microstructural changes in the association, projection, and commissural compact white matter pathways of the human brain over the lifespan in a cohort of healthy right-handed children and adults aged 6–68 years. In both males and females, the diffusion tensor radial diffusivity of the bilateral arcuate fasciculus, inferior longitudinal fasciculus, inferior fronto-occipital fasciculus, uncinate fasciculus, corticospinal, somatosensory tracts, and the corpus callosum followed a U-curve with advancing age; fractional anisotropy in the same pathways followed an inverted U-curve. Our study provides useful baseline data for the interpretation of data collected from patients.

Keywords

Lifespan; White matter fiber tract development; Association; Projection; Commissural pathways; Aging; Nonlinear trajectories; Diffusion tensor imaging; Tractography

Introduction

The noninvasive mapping and quantification of human brain white matter micro- and macro-structural changes remain challenging endeavors in both health and disease (Crick and Jones 1993; Filley 2001). The availability of normative quantitative baseline data would help advance our knowledge about brain–behavior relations. These data would also facilitate clinical interpretation of changes in brain structure during transitional stages from childhood to adulthood to senescence when the brain is at high risk of developing age-related pathologies (Yakovlev and Lecours 1967; Caviness et al. 1996; Paus et al. 1999; Courchesne et al. 2000; Filley 2001; Sowell et al. 2003; Charlton et al. 2006; Jernigan and Fennema-Notestine 2004; Lenroot and Giedd 2006).

Correspondence to: Khader M. Hasan.

Electronic supplementary material The online version of this article (doi:10.1007/s00429-009-0238-0) contains supplementary material, which is available to authorized users.

Magnetic resonance imaging (MRI) of water molecular motional degrees of freedom such as rotation, vibration, and random translation have been utilized in the past 2 decades to identify milestones of human white and gray matter development (Paus et al. 1999; Courchesne et al. 2000; Sowell et al. 2003; Le Bihan 2003). MRI tissue contrast has offered compartmental volumes utilized to shed light into issues such as effects of hemispheric lateralization, sex, and age as well as their interaction with pathology, training, and environment. There is minimal noninvasive literature characterizing white matter morphological and morphometric changes across the entire human lifespan (Allen et al. 1991; Pujol et al. 1993; Courchesne et al. 2000; Sowell et al. 2003; Walhovd et al. 2005).

Diffusion tensor imaging (DTI) provides metrics that have been used to map the architecture of deep central nervous system tissue connectivity in vivo (Basser 1997; Le Bihan 2003; Behrens et al. 2003). DTI scalar metrics such as fractional anisotropy (FA) can be related to the ratio of diffusivity along relative to that perpendicular to compact fibers (Hasan and Narayana 2006). In general, hindrances to water molecular diffusion between axons have been associated with the degree of myelination (Beaulieu 2002; Song et al. 2005).

DTI-derived metrics have been used in hundreds of publications to provide surrogate markers of development (Mukherjee and McKinstry 2006), aging (Gong et al. 2009; Zahr et al. 2009) and pathology (Ewing-Cobbs et al. 2008). Due to rapidly changing acquisition and analysis methods, the quantitative results of several DTI studies conducted in small populations with different age groups seem contradictory even on well-organized and coherent white matter structures such as the posterior limb of internal capsule (pLIC) and corpus callosum (CC). Studying the effects of age, sex, and lateralization on tissue integrity remains challenging, and may require large populations to accommodate sampling and individual variability (Hasan et al. 2009a, b; Lebel et al. 2008; Stadlbauer et al. 2008; Sullivan et al. 2009; Zahr et al. 2009). For example, using healthy controls and a region-of-interest (ROI) methodology, Snook et al. (2005) showed that FA (pLIC) increases significantly with age in a cohort 5–27 years with no sex or lateralization effects. Abe et al. (2000) reported that the FA (pLIC) was age, sex, and hemisphere independent. In contrast, Salat et al. (2005) and Ardekani et al. (2007) showed slight lateralization effects FA (pLIC Left > pLIC Right) with a steady age decrease from young adulthood to middle age. Using voxel-based analysis (VBA), Park et al. (2004) reported significant lateralization of FA in the adult pLIC (Right > Left). Chepuri et al. (2002) reported that the regional corpus callosum diffusion anisotropy was heterogeneous and showed neither gender nor age effects, whereas other investigators reported that the genu CC anisotropy decreased with age while the splenium CC anisotropy did not alter with age (Abe et al. 2000; Salat et al. 2005). Recent quantitative work on the CC using diffusion tensor fiber tracking (DT-FT) (Ota et al. 2006; Sullivan et al. 2006) showed that diffusion anisotropy decreased more rapidly with age in the anterior callosal fibers than in the posterior fibers in both men and women.

To the best of our knowledge, there are no quantitative lifespan studies that examined the effects of age, gender, and lateralization using multiple DTI metrics of the association (Makris et al. 1997; Mori et al. 2002; Catani et al. 2002, 2005), projection (Berman et al. 2005), and commissural pathways (Xu et al. 2002) in both children (Eluvathingal et al. 2007), adolescents (Lebel et al. 2008), young and older adults (Hasan et al. 2009a, b; Stadlbauer et al. 2008; Sullivan et al. 2009). There seems to be a scant amount of DTI literature on the aging of the association pathways such as the arcuate fasciculus and uncinate fasciculus (Hasan et al. 2009b) in adults. The importance of age as a major confounding factor has been pointed out by Jones et al. (2006) and Head et al. (2004) in the context of interpretation of DTI data collected from adult schizophrenia and older dementia patients, respectively.

In this work, we present the results of quantitative DTI fiber tractography measurements of the human brain pathways in a large cohort of developing right-handed children (age-matched boys and girls), and young and older adults (age-matched men and women). We hypothesized that nonlinear curves would best represent age-related changes in the compact white matter fiber tracts. We also examined whether anisotropy and/or radial diffusivity varied according to sex and cerebral hemisphere.

Materials and methods

Participants

The participants included a cohort of 119 healthy right-handed children and adults recruited in the past 3 years for different studies at our institution to provide a quantitative baseline for the interpretation of patient data. The participants included 42 developing children and adolescents (22 boys: age range = 6.9–16.7; mean ± SD = 11.7 ± 3.2 years; 20 girls: age range = 6.9–18.7; mean ± SD = 10.3 ± 2.9 years), in addition to 77 young/middle age/older men and women (32 men: age range = 19–68.3, mean ± SD = 36.7 ± 13.5 and 45 women: age range = 20.3–67, mean ± SD = 38 ± 13.5). In the whole sample, there were no mean age differences between the 54 males (age mean ± SD = 26.5 ± 16.2) and 65 females (age mean ± SD = 29.5 ± 17.2) ($p = 0.34$). The demographic and inclusion details for each tract studied are provided in the Supplementary Methods.

Healthy adults were recruited from the local community to help in the interpretation of brain MRI quantitative data collected from patients (Ewing-Cobbs et al. 2008; Hasan et al. 2009d). All adults were screened using a questionnaire for history of head trauma, brain surgery, chronic illness, alcohol and/or drug abuse, neurological illness, and for current pregnancy. Healthy children were recruited as detailed elsewhere (Ewing-Cobbs et al. 2008). Children included satisfied three criteria (1) no known premorbid neurologic or metabolic disorder, (2) no history of prior traumatic brain injury, and (3) gestational age >30 weeks. All MRI structural scans were read as “normal” by a board certified radiologist (LAK).

Written informed consent was obtained from the adults and guardians of children and adolescents; assent was also obtained from the children/adolescents participating in these studies per the University of Texas Health Science Center at Houston institutional review board regulations for the protection of human research subjects.

MRI and DTI data acquisition, processing and quality control

The data were collected from all participants using a 3T Philips Intera scanner (Philips Medical Systems, Best, The Netherlands), equipped with parallel imaging technology. Additional details on the DTI data analysis are provided elsewhere (Hasan et al. 2009a, b).

Diffusion-weighted data acquisition—The diffusion-weighted image (DWI) data were acquired using a single-shot spin echo diffusion sensitized echo-planar imaging (EPI) sequence with the balanced *Icosa21* encoding scheme (Hasan and Narayana 2003), a diffusion sensitization of b = 1,000 s mm^{-2}, repetition time $T_R = 6.1$ s, and echo time $T_E = 84$. The slice thickness was 3 mm with 44 axial slices covering the entire brain (foramen magnum to vertex), a square field-of-view = 240 × 240 mm^2, and an image matrix of 256 × 256 (Eluvathingal et al. 2007). The total DWI acquisition time was approximately 7 min and resulted in accurate and reproducible DTI metric estimation (Conturo et al. 1995; Pierpaoli et al. 1996; Eluvathingal et al. 2007). Scanner temporal stability and DTI quality control over the span of data acquisition were assured using same subject and water phantom tests as detailed elsewhere (Hasan 2007).

DTI data processing—The DWI data were intra-registered to the baseline "b_0" images (without diffusion weighting) to correct for the eddy-current image distortions in each of the 21 diffusion-weighted volumes using a mutual information approach (Netsch and van Muiswinkel 2004). The diffusion-weighed data were decoded to obtain the diffusion tensors (Le Bihan 1995). The diffusion tensors are then diagonalized to provide the tensor eigenvectors and eigenvalues (Johansen-Berg and Behrens 2009; Le Bihan 1995; Mori 2007).

DTI metrics—The DTI-derived metrics used are the radial (λ_t) and the axial ($\lambda_{||} = \lambda_1$) diffusivities. The radial diffusivity was defined as the mean of the medium (λ_2), and minor (λ_3) eigenvalues ($\lambda_t = \lambda_\perp = (\lambda_2 + \lambda_3)/2$). The fractional anisotropy (FA) is computed using the eigenvalues according to Eq. 1:

$$\mathrm{FA} = \sqrt{\frac{1}{2}\frac{(\lambda_1 - \lambda_2)^2 + (\lambda_2 - \lambda_3)^2 + (\lambda_1 - \lambda_3)^2}{\lambda_1^2 + \lambda_2^2 + \lambda_3^2}} \quad (1)$$

The radial and axial diffusivities ($\lambda_\perp$ and $\lambda_{||}$) have been shown in animal models of human disease to provide a more specific interpretation of DTI results than provided by FA and the mean diffusivity (Song et al. 2005).

Diffusion tensor imaging fiber tracking—Compact WM fiber tracking of association, projection and commissural pathways (Aralasmak et al. 2006; Huang et al. 2005; Wakana et al. 2004) was performed using DTI Studio software (H. Jiang and S. Mori; Johns Hopkins University, Baltimore, MD, USA; http://www.cmrm.med.jhmi.edu) based on Fiber Assignment by Continuous Tracking algorithm (Mori et al. 2002; Jiang et al. 2006).

The association pathways were studied bilaterally (see Fig. 1) and included the arcuate fasciculus (AF) (Catani et al. 2002,2005;Nucifora et al. 2005;Powell et al. 2006;Eluvathingal et al. 2007). The arcuate fasciculus was divided into three segments: frontotemporal-AFT, fronto-parietal-AFP, temporopareital-ATP, as described elsewhere (Eluvathingal et al. 2007). The association pathways also included the inferior longitudinal fasciculus (ILF), inferior fronto-occipital fasciculus (IFOF), and uncinate fasciculus (UF) (Rodrigo et al. 2007;Hasan et al. 2009b). The projection pathways included bilateral corticospinal (CST) and somatosensory (SS) pathways (Berman et al. 2005;Dubois et al. 2006;Eluvathingal et al. 2007) (see Fig. 1). For the commissural pathways we adapted the Witelson–Aboitiz approach, to divide the corpus callosum (CC) into eight functionally specialized sectors that connect the homologous areas of frontal, temporal, orbital, parietal and occipital cortices (de Lacoste et al. 1985;Aboitiz et al. 1992;Hasan et al. 2009a). A total of 24 pathways (16 intrahemispheric, 8 commissural) were quantified. These pathways are specialized in interhemispheric cognitive and motor functions, speech and language (AF), motor (CST), and somatosensory functions (SS). Brute force tractography and multiple ROI technique were utilized to trace the white matter pathway of interest (Conturo et al. 1999). The association and projection pathways included in the present study were traced based on established fiber tracking methods detailed elsewhere (Eluvathingal et al. 2007;Hasan et al. 2009b). Additional details on the commissural pathways are provided in the Supplementary Methods (see also Hasan et al. 2009a).

Statistical analysis

DTI metrics were analyzed using generalized linear models with effects age and sex as between-subjects variables. Given previous reports (Allen et al. 1991; Courchesne et al. 2000; Sowell et al. 2003; Hasan et al. 2007, 2009a, b; Lebel et al. 2008; McLaughlin et al. 2007), both linear and quadratic (nonlinear) age terms were included. The DTI metrics (e.g., FA, radial diffusivity) were modeled as $y = \beta_0 + \beta_1 \times \mathrm{age} + \beta_2 \times \mathrm{age}^2$, then the general least-

squares methods were used to compute the coefficients, standard errors, and their statistical significance upon comparing males and females. Interactions of sex with age (both terms) were examined, and trimmed where non-significant. If the quadratic age term was not significant, age and sex interactions were examined without this term, and trimmed if non-significant. The age at peak and its standard deviation were computed (Glantz 2002) assuming significant linear and quadratic terms using Eq 2:

$$\frac{dy}{dAge}=0 \Rightarrow A_p=-\frac{\beta_1}{2\beta_2} \iff \frac{\sigma(A_p)}{A_p} = \sqrt{\left(\frac{\sigma(\beta_1)}{\beta_1}\right)^2+\left(\frac{\sigma(\beta_2)}{\beta_2}\right)^2}. \quad (2)$$

Hemispheric diffusion asymmetry (Peled et al. 1998) [i.e., FA (Right) vs. FA (Left)] of the association and projection tracts was examined for children, adults, and by gender (boys and men; girls and women) using paired *t* tests. Significant main effects for age were followed up with paired comparisons controlling for multiple comparisons to hold the alpha level at 0.05. All statistical analyses were conducted using SAS 9.1 (SAS Institute Inc, NC) and MATLAB R12.1 Statistical Toolbox v 3.0 (The Mathworks Inc, Natick, MA, USA).

Results

Tables 1 and 2, and the corresponding Figs. 2a–d and 3a–d summarize the quadratic least-squares fitted FA and radial diffusivity results as function of age for (a) the three right and left arcuate fasciculus segments (ATP, AFP and AFT) (b) the bilateral ILF, IFO, and UF (c) the bilateral corticospinal and somatosensory pathways, and (d) the commissural pathways (CC1–CC8) (see also Supplementary Results for the corresponding axial diffusivity ($\lambda_{||}$) tabulated values and plots). The best fit parameters, their corresponding standard deviations ($\beta \pm \sigma(\beta)$), and statistical significance (p) are listed along with the age at peak as described in the "Methods". The age statistics and population numbers used for each tract is detailed in the Supplementry Methods.

Microstructural DTI heterogeneity of white matter pathways

In general, all tracts exhibit unique diffusivities and FA values. The corpus callosum most posterior sector tracts (CC8) exhibited the largest FA (Fig. 2). The left corticospinal tract has the second largest FA attributable mostly to low average values of radial diffusivity (Fig. 3). It is noted that amongst all association pathways studied, the fronto-temporal segment of the arcuate fasciculus (AFT) has the lowest radial diffusivity at all ages.

Age effects

Note the unique spatial heterogeneity and temporal variation of all the measured white matter tracts, which reflect the microstructural development and functional specialization subserved by these tracts (Zahr et al. 2009). Fractional anisotropy followed an inverted U-curve (Table 1, Fig. 2), whereas the radial diffusivity followed a quadratic or U-curve for all pathways in both males and females (Table 2, Fig. 3).

Sex effects

In general, there were minimal and non-significant sex effects on the DTI-derived metrics in all tracts studies. The ILF is the only tract that exhibited significant ($p < 0.05$) sex-by-hemispheres effects (e.g. Left >Right and Males > Females; see Supplementary Results for details).

Asymmetry and lateralization effects

Hemispheric lateralization effects were examined for children and adults in the association and projection pathways by comparing FA mean values in the bilateral fiber tracts. The FA index has been used to assess tract lateralization in our previous study in right-handed children and adolescents (Eluvathingal et al. 2007) as well as almost all DTI studies that reported lateralization. Fractional anisotropy values for the divisions of the arcuate, showed significant R >L asymmetry in the child group only for the frontoparietal segment (AFP). Adults had R >L for both the ATP and AFP segments. Regarding the other association pathways, only the uncinate fasciculus showed asymmetry in children, with L >R. In adults, FA was significantly greater on the right for the ILF and on the left for the UF. For projection pathways, FA of the CST and SS was similar across hemispheres for children. For adults, FA was greater in the left than right CST; values were similar in the SS (see Supplementary Results for details).

Discussion

In this report, we used noninvasive DTI fiber tracking methods to map the white matter bundles (Wakana et al. 2004) across the human lifespan (Hasan et al. 2007, 2009a, b). In animal models using histology and neurophysiological measurements, scalar metrics such as the radial diffusivity have correlated with myelination (Beaulieu 2002; Drobyshevsky et al. 2005; Song et al. 2005). Our previous DTI study in children (Eluvathingal et al. 2007) as well as several others (see Hasan et al. 2009a, b for review) has shown the utility and sensitivity of the radial diffusivity in following the developmental aspects of white matter tracts.

Fiber tract DTI heterogeneity

Our results on the FA heterogeneity of the association, projection, and commissural pathways are consistent with previous voxel-based morphometric MRI (Paus et al. 1999), histological (Highley et al. 1999, 2002; Aboitiz et al. 1992; LaMantia and Rakic 1990; Terao et al. 1994), and recent DTI studies that show regional variation in white matter and fiber microstructure (Park et al. 2004; Partridge et al. 2004; Vernooij et al. 2007; Hasan et al. 2009a, b; Hermoye et al. 2006). Lower radial diffusivity may reflect higher myelin thickness which may be associated with large myelinated axons that require fast conduction like the CST (see Table 2; Fig. 3). Large caliber and myelinated fibers have been documented to populate the middle and posterior sectors of the corpus callosum (e.g. CC4, CC8) (LaMantia and Rakic 1990; Aboitiz et al. 1992). These fibers facilitate a high level of synchrony between the two hemispheres and support interhemispheric signal communication for motor, auditory, and visual tasks (Aboitiz et al. 1992). Less myelinated or small caliber fibers commonly found in the frontal lobe (e.g. CC1) (Bartzokis et al. 2001) and in sensory pathways (Filley 2001) would be expected to have larger radial diffusivity as water molecules encounter fewer obstacles to diffusion. Our quantitative data (Figs. 2, 3 and Tables 1, 2) are consistent with this general qualitative assessment (i.e., FA (CST) > FA (SS)).

Age effects

Several studies including our previous work in children (Eluvathingal et al. 2007) have used linear age curves to characterize the developmental trends observed in normally developing children. Our current work shows that upon including younger and older adults, nonlinear trends are more appropriate to account for the age-related variability for ages 6–68 years. Nonlinear curves have been previously used to model the variation of lobar cortical or white matter volume with advancing age (Courchesne et al. 2000; Bartzokis et al. 2001; Sowell et al. 2003). A few lifespan studies have also shown the age trajectories of gray matter nuclei (Walhovd et al. 2005) and the midsagittal corpus callosum area (Allen et al. 1991; Pujol et al. 1993). Our study provides microstructural correlates of such macroscopic changes in white matter volume or area as a result of neuronal, dendrite or axonal loss, demyelination and

Wallerian degeneration (Masliah et al. 1993; Pakkenberg and Gundersen 1997; Sowell et al. 2003; Bartzokis et al. 2007). In general, most compact white matter tracts attained radial diffusivity minimum in the third to fourth decade for both males and females, reflecting continued "progressive" myelination post-adolescence (Yakovlev and LeCours 1967; Bartzokis et al. 2001; Courchesne et al. 2000; Sowell et al. 2003) with declines in subsequent decades associated with "regressive and degenerative" natural aging.

Our study consolidates several independent DTI publications on the association, projection and commissural pathways in children, young (Eluvathingal et al. 2007; Lebel et al. 2008) and older adults (Hasan et al. 2009a, b). In particular, the significant nonlinear age trajectories (Figs. 2, 3) reconcile the published trends on the CST (Snook et al. 2005; Westerhausen et al. 2007) and CC (Ota et al. 2006; McLaughlin et al. 2007). It can be inferred that the posterior section (splenium) of the corpus callosum undergoes an increase in diffusion anisotropy starting in utero (Bui et al. 2006) which was also observed in neonates (Dubois et al. 2006) and in children and adolescents (Mukherjee et al. 2002; Snook et al. 2005). The trend in young adults shows a plateau and then a slow decline with age as shown by studies in young (Snook et al. 2005), old (Sullivan et al. 2006; Ota et al. 2006) and aging adults (Head et al. 2004).

Our study is the first to provide nonlinear age trajectories across the lifespan of the arcuate fasciculus and CST tracts which are the two most-studied tracts. Previous studies using voxel-based MRI methods (Paus et al. 1999) in children and adolescents showed a steady increase in white matter density; our study shows age-related impairment of the microstructural integrity of these tracts as measured by FA and the radial diffusivity.

Sex effects

We found minimal effects of sex on all tracts studied. In particular, the CC regional FA and radial diffusivity were not sex-dependent. Our results are consistent with several DTI publications that did not report sex-differences (Chepuri et al. 2002; Abe et al. 2000; Hasan et al. 2009a; Lebel et al. 2008; Ota et al. 2006). There are a few studies that reported significant FA (men) > FA (women) (Shin et al. 2005; Westerhausen et al. 2004) for all sectors of the midsagittal corpus callosum, while one study reported a leftward frontal asymmetry in women and FA (women) >FA (men) (Szeszko et al. 2003). Due to methodological and population-related issues, we could not comment on the main reasons for such discrepancies.

The present study gives a microstructural basis for the earlier volumetry reports of sex-independent regional white matter reduction with aging that follow an inverted U-curve (Courchesne et al. 2000; Allen et al. 1991). Continued loss of myelin and impaired remyelination can contribute to the accumulated volume loss (Bartzokis et al. 2007). Possible subtle sex-based differences may as well be dependent on several factors including genetic, hormonal activity, and accumulated free radicals such as iron (Bartzokis et al. 2007).

Asymmetry and hemispheric lateralization effects

In our studies FA (Right AFP) was found significantly greater than FA (Left AFP) at all ages for both males and females. The ATP segment of the arcuate showed rightward asymmetry trend in adults only, while the AFT segment did not show asymmetry using FA in both children and adults. Previous conventional MRI studies (Paus et al. 1999) and several DTI studies (Nucifora et al. 2005; Powell et al. 2006; Vernooij et al. 2007) have reported sex-independent leftward asymmetry in right-handed adults (Vernooij et al. 2007). Only one study (Park et al. 2004) reported rightward asymmetry in the superior and straight segment of the arcuate as reported in the current study.

The FA in the Left UF was found slightly larger than the Right UF; this is consistent with recent reports in children (Eluvathingal et al. 2007) and adults (Hasan et al. 2009b). Previous studies on the UF (see more details in Hasan et al. 2009b) showed a leftward FA asymmetry trend (Kubicki et al. 2002) using an ROI approach, while Park et al. (2004) showed that the superior section of the UF is leftward asymmetric and the inferior is rightward asymmetric. A recent DTI study by Rodrigo et al. (2007) showed a rightward asymmetry as has also been reported in older adults by Highley et al. (1999), while Taoka et al. (2006) reported diffusion anisotropy symmetry in the UF.

In this study, we report a leftward sex-independent FA asymmetry or FA (Left CST) > FA (Right CST) in adults and FA (Left) ~ FA (Right) in children. The CST asymmetry is controversial in published DTI literature. For example, Nucifora et al. (2005) and Ciccarelli et al. (2003) did not report asymmetry. Region-of-interest DTI studies on the posterior limb of the internal capsule show further discrepancies. There are reports of FA no asymmetry in adults (Abe et al. 2000) and in children (Snook et al. 2005), a rightward asymmetry (Park et al. 2004) and leftward asymmetry in adults (Salat et al. 2005; Ardekani et al. 2007).

Age, sex and diffusion asymmetry interactions

The SS exhibited some sex-by-hemisphere interactions in women only (FA (Left > Right), $p = 0.02$; see Fig. 2). The ILF FA asymmetry (Right > Left) was stronger in men ($p < 0.0001$) than in women ($p = 0.01$). The published data on the aging, sex and asymmetry of the ILF in adults is scant. A rightward FA asymmetry (Right > Left) of the ILF observed in this study in both men and women has been reported previously in healthy men (Park et al. 2004).

The interpretation of the meaning of regional lateralization, age, and sex interactions using DTI should be approached with caution in view of limited preliminary DTI reports and rapidly improving methods (Szeszko et al. 2003; Westerhausen et al. 2004; Shin et al. 2005). The traditional structural hemispheric lateralization concept is based on gray matter lobar volumes or weights as assessed in postmortem studies. White matter fiber tracks (e.g., uncinate fasciculus) may traverse different lobes and hence their DTI-based microstructural asymmetry may be region-dependent, and hence DTI-regional asymmetry does not necessarily relate to the gross anatomical or volume cerebral asymmetry (Good et al. 2001; Allen et al. 2003; Luders et al. 2006; Westerhausen et al. 2007; Vernooij et al. 2007).

Sex-based DTI asymmetries should also be interpreted with caution as DTI measures reflect regional neuronal and axonal organization which could be dependent on several variables including function and hormonal activity. It has been proposed by Allen et al. (2003) that axonal geometry may not be “sexually dimorphic” and hence DTI measurements at the current levels of signal-to-noise ratio and spatial resolution may reflect an insensitive measure to sex-related variations.

In general, white matter visible on MRI is composed of packed axons with function-space dependent myelin and caliber distribution. White matter also contains glial cells (e.g., oligodendrocytes and astrocytes), and blood vessels (Filley 2001). A comprehensive interpretation of in vivo DTI measurements in terms of all possible signal contributors has not been presented yet (Beaulieu 2002; Pierpaoli et al. 1996) and the only clues have been provided by combined DTI and histology measurements using animal studies on structures such as the corpus callosum and spinal cord (Song et al. 2005; Schwartz et al. 2005). Also, to the best of our knowledge there have been no lifespan postmortem histological cross-sectional studies in humans even on structures such as the corpus callosum, uncinate fasciculus, and corticospinal tracts which are known to be extremely heterogeneous from a few and limited postmortem studies on the adult corpus callosum (Aboitiz et al. 1992; Highley et al. 1999), uncinate fasciculus (Highley et al. 1999) and corticospinal tract (Terao et al. 1994).

Limitations, future plans and conclusion

Our study underscores the importance of using nonlinear age models when analyzing DTI data in children and adults. The DTI acquisition protocol was maintained for ~3 years and was subjected to extensive quality control measures. Although our study may be one of the largest DTI cross-sectional studies to-date on right-handed males and females aged 6–68 years, we should also point out that a longitudinal quantitative DTI study will be more challenging to design as DTI technology and protocols advance rapidly. Our database is being extended using a larger control pediatric and adult populations that will help us further investigate important topics such as remyelination (Peters and Sethares 2003; Bartzokis et al. 2007), and the interplay between complex issues such as sex, handedness, and function. A future extension of the current studies will consider the spatiotemporal dynamics of cortical and gray matter (Hasan et al. 2009c; Makris and Pandya 2009) that accompanies the progressive and regressive changes in white matter connectivity.

In conclusion, we demonstrated that the diffusion tensor derived metrics such as FA and radial diffusivity can detect changes in the microstructural organization of the human brain white matter pathways across the human lifespan. Age-related DTI changes follow nonlinear curves and may provide noninvasive surrogate markers for changes in human behavior and cognition (Zahr et al. 2009) in health and disease.

Supplementary Material

Refer to Web version on PubMed Central for supplementary material.

Acknowledgments

This work is funded by NIH R01 NS052505-04 awarded to KMH, NINDS R01 NS046308 awarded to LEC and P01 HD35946 awarded to JMF. The assistance of Vipul Kumar Patel in data acquisition is appreciated.

Abbreviations

A	Adults
AF	Arcuate fasciculus
B	Boys
C	Children
CC	Corpus callosum
CST	Corticospinal tract
DTI	Diffusion tensor imaging
DTT	Diffusion tensor tractography
DT-FT	Diffusion tensor fiber tracking
G	Girls
gCC	Genu of the corpus callosum
FA	Fractional anisotropy
AFP	Fronto-parietal segment of arcuate fasciculus
AFT	Fronto-temporal segment of arcuate fasciculus
IFOF	Inferior fronto-occipital fasciculus

ILF	Inferior longitudinal fasciculus
L	Left
M	Men
MRI	Magnetic resonance imaging
pLIC	Poster limb of internal capsule
R	Right
ROI	Region-of-interest
SNR	Signal-to-noise ratio
sCC	Splenium of the corpus callosum
SS	Somatosensory pathway
ATP	Temporo-parietal segment of arcuate fasciculus
UF	Uncinate fasciculus
VBA	Voxel-based analysis
W	Women

References

Abe O, Aoki S, Hayashi N, Yamada H, Kunimatsu A, Mori H, Yoshikawa T, Okubo T, Ohtomo K. Normal aging in the central nervous system: quantitative MR diffusion-tensor analysis. Neurobiol Aging 2000;23:433–441. [PubMed: 11959406]

Aboitiz F, Scheibel AB, Fisher RS, Zaidel E. Fiber composition of the human corpus callosum. Brain Res 1992;598:143–153. [PubMed: 1486477]

Allen LS, Richey MF, Chai YM, Gorski RA. Sex differences in the corpus callosum of the living human being. J Neurosci 1991;11:933–942. [PubMed: 2010816]

Allen JS, Damasio H, Grabowski TJ, Bruss J, Zhang W. Sexual dimorphism and asymmetries in the gray-white composition of the human cerebrum. NeuroImage 2003;18:880–894. [PubMed: 12725764]

Aralasmak A, Ulmer JL, Kocak M, Salvan CV, Hillis AE, Yousem DM. Association, commissural, and projection pathways and their functional deficit reported in literature. J Comput Assist Tomogr 2006;30:695–715. Review. [PubMed: 16954916]

Ardekani S, Kumar A, Bartzokis G, Sinha U. Exploratory voxel based analysis of diffusion indices and hemispheric asymmetry in normal aging. Magn Reson Imaging 2007;25:154–167. [PubMed: 17275609]

Bartzokis G, Beckson M, Lu PH, Nuechterlein KH, Edwards N, Mintz J. Age-related changes in frontal and temporal lobe volumes in men: a magnetic resonance imaging study. Arch Gen Psychiatry 2001;58:461–465. [PubMed: 11343525]

Bartzokis G, Tishler TA, Lu PH, Villablanca P, Altshuler LL, Carter M, Huang D, Edwards N, Mintz J. Brain ferritin iron may influence age- and gender-related risks of neurodegeneration. Neurobiol Aging 2007;28:414–423. [PubMed: 16563566]

Basser PJ. New histological and physiological stains derived from diffusion-tensor MR images. Ann NY Acad Sci 1997;820:123–138. [PubMed: 9237452]

Beaulieu C. The basis of anisotropic water diffusion in the nervous system—a technical review. NMR Biomed 2002;15:435–455. [PubMed: 12489094]

Behrens TE, Johansen-Berg H, Woolrich MW, Smith SM, Wheeler-Kingshott CA, Boulby PA, Barker GJ, Sillery EL, Sheehan K, Ciccarelli O, Thompson AJ, Brady JM, Matthews PM. Non-invasive mapping of connections between human thalamus and cortex using diffusion imaging. Nat Neurosci 2003;6:750–757. [PubMed: 12808459]

Berman JI, Mukherjee P, Partridge SC, Miller SP, Ferriero DM, Barkovich AJ, Vigneron DB, Henry RG. Quantitative diffusion tensor MRI fiber tractography of sensorimotor white matter development in premature infants. Neuroimage 2005;27:862–871. [PubMed: 15978841]

Bui T, Daire JL, Chalard F, Zaccaria I, Alberti C, Elmaleh M, Garel C, Luton D, Blanc N, Sebag G. Microstructural development of human brain assessed in utero by diffusion tensor imaging. Pediatr Radiol 2006;36:1133–1140. [PubMed: 16960686]

Catani M, Howard RJ, Pajevic S, Jones DK. Virtual in vivo interactive dissection of white matter fasciculi in the human brain. NeuroImage 2002;17:77–94. [PubMed: 12482069]

Catani M, Jones DK, Ffytche DH. Perisylvian language networks of the human brain. Ann Neurol 2005;57:8–16. [PubMed: 15597383]

Caviness VS Jr, Kennedy DN, Richelme C, Rademacher J, Filipek PA. The human brain age 7–11 years: a volumetric analysis based on magnetic resonance images. Cereb Cortex 1996;6:726–736. [PubMed: 8921207]

Charlton RA, Barrick TR, McIntyre DJ, Shen Y, O'Sullivan M, Howe FA, Clark CA, Morris RG, Markus HS. White matter damage on diffusion tensor imaging correlates with age-related cognitive decline. Neurology 2006;66:217–222. [PubMed: 16434657]

Chepuri NB, Yen YF, Burdette JH, Li H, Moody D, Maldjian JA. Diffusion anisotropy in the corpus callosum. Am J Neuroradiol 2002;23:803–808. [PubMed: 12006281]

Ciccarelli O, Parker GJ, Toosy AT, Wheeler-Kingshott CA, Barker GJ, Boulby PA, Miller DH, Thompson AJ. From diffusion tractography to quantitative white matter tract measures: a reproducibility study. Neuroimage 2003;18:348–359. [PubMed: 12595188]

Conturo TE, McKinstry RC, Aronovitz JA, Neil JJ. Diffusion MRI: precision, accuracy and flow effects. NMR Biomed 1995;8:307–332. [PubMed: 8739269]

Conturo TE, Lori NF, Cull TS, Akbudak E, Snyder AZ, Shimony JS, McKinstry RC, Burton H, Raichle ME. Tracking neuronal fiber pathways in the living human brain. Proc Natl Acad Sci USA 1999;96:10422–10427. [PubMed: 10468624]

Courchesne E, Chisum HJ, Townsend J, Cowles A, Covington J, Egaas B, Harwood M, Hinds S, Press GA. Normal brain development and aging: quantitative analysis at in vivo MR imaging in healthy volunteers. Radiology 2000;216:672–682. [PubMed: 10966694]

Crick F, Jones E. Backwardness of human neuroanatomy. Nature 1993;361:109–110. [PubMed: 8421513]

de Lacoste MC, Kirkpatrick JB, Ross ED. Topography of the human corpus callosum. J Neuropathol Exp Neurol 1985;44:578–591. [PubMed: 4056827]

Drobyshevsky A, Song SK, Gamkrelidze G, Wyrwicz AM, Derrick M, Meng F, Li L, Ji X, Trommer B, Beardsley DJ, Luo NL, Back SA, Tan S. Developmental changes in diffusion anisotropy coincide with immature oligodendrocyte progression and maturation of compound action potential. J Neurosci 2005;25:5988–5997. [PubMed: 15976088]

Dubois J, Hertz-Pannier L, Dehaene-Lambertz G, Cointepas Y, Le Bihan D. Assessment of the early organization and maturation of infants' cerebral white matter fiber bundles: a feasibility study using quantitative diffusion tensor imaging and tractography. Neuroimage 2006;30:1121–1132. [PubMed: 16413790]

Eluvathingal TJ, Hasan KM, Kramer L, Fletcher JM, Ewing-Cobbs L. Quantitative diffusion tensor tractography of association and projection fibers in normally developing children and adolescents. Cereb Cortex 2007;17:2760–2768. [PubMed: 17307759]

Ewing-Cobbs L, Prasad MR, Swank P, Kramer L, Cox CS Jr, Fletcher JM, Barnes M, Zhang X, Hasan KM. Arrested development and disrupted callosal microstructure following pediatric traumatic brain injury: relation to neurobehavioral outcomes. Neuroimage 2008;42:1305–1315. [PubMed: 18655838]

Filley, CM. The behavioral neurology of white matter. Oxford; New York: 2001.

Glantz, SA. Primer of biostatistics. 5. McGraw-Hill; New York: 2002.

Gong G, He Y, Concha L, Lebel C, Gross DW, Evans AC, Beaulieu C. Mapping anatomical connectivity patterns of human cerebral cortex using in vivo diffusion tensor imaging tractography. Cereb Cortex 2009;19:524–536. [PubMed: 18567609]

Good CD, Johnsrude I, Ashburner J, Henson RNA, Friston KJ, Frackowiak RSJ. Cerebral asymmetry and the effects of sex and handedness on brain structure: a voxel-based morphometric analysis of 465 normal adult human brains. NeuroImage 2001;14:685–700. [PubMed: 11506541]

Hasan KM. A framework for quality control and parameter optimization in diffusion tensor imaging: theoretical analysis and validation. Magn Reson Imaging 2007;25:1196–1202. [PubMed: 17442523]

Hasan KM, Narayana PA. Computation of the fractional anisotropy and mean diffusivity maps without tensor decoding and diagonalization: Theoretical analysis and validation. Magn Reson Med 2003;50:589–598. [PubMed: 12939767]

Hasan KM, Narayana PA. Retrospective measurement of the diffusion tensor eigenvalues from diffusion anisotropy and mean diffusivity in DTI. Magn Reson Med 2006;56:130–137. [PubMed: 16755537]

Hasan KM, Sankar A, Halphen C, Kramer LA, Brandt ME, Juranek J, Cirino PT, Fletcher JM, Papanicolaou AC. Ewing-Cobbs Development and organization of the human brain tissue compartments across the lifespan using diffusion tensor imaging. Neuroreport 2007;18:1735–1739. [PubMed: 17921878]

Hasan KM, Kamali A, Iftikhar A, Kramer LA, Papanicolaou AC, Fletcher JM, Ewing-Cobbs L. Diffusion tensor tractography quantification of the human corpus callosum fiber pathways across the lifespan. Brain Res 2009a;1249:91–100. [PubMed: 18996095]

Hasan KM, Iftikhar A, Kamali A, Kramer LA, Ashtari M, Cirino PT, Papanicolaou AC, Fletcher JM, Ewing-Cobbs L. Development and aging of the healthy human brain uncinate fasciculus across the lifespan using diffusion tensor tractography. Brain Res 2009b;1276:67–76. [PubMed: 19393229]

Hasan KM, Kamali A, Kramer LA. Mapping the human brain white matter tracts relative to cortical and deep gray matter using diffusion tensor imaging at high spatial resolution. Magn Reson Imaging 2009c;27:631–636. [PubMed: 19128910]

Hasan KM, Halphen C, Kamali A, Nelson FM, Wolinsky JS, Narayana PA. Caudate nuclei volume, diffusion tensor metrics, and T2 relaxation in healthy adults and relapsing-remitting multiple sclerosis patients: implications for understanding gray matter degeneration. J Magn Reson Imaging 2009d; 29:70–77. [PubMed: 19097116]

Head D, Buckner RL, Shimony JS, Williams LE, Akbudak E, Conturo TE, McAvoy M, Morris JC, Snyder AZ. Differential vulnerability of anterior white matter in nondemented aging with minimal acceleration in dementia of the Alzheimer type: evidence from diffusion tensor imaging. Cereb Cortex 2004;14:410–423. [PubMed: 15028645]

Hermoye L, Saint-Martin C, Cosnard G, Lee SK, Kim J, Nassogne MC, Menten R, Clapuyt P, Donohue PK, Hua K, Wakana S, Jiang H, van Zijl PC, Mori S. Pediatric diffusion tensor imaging: normal database and observation of the white matter maturation in early childhood. NeuroImage 2006;29:493–504. [PubMed: 16194615]

Highley JR, Esiri MM, McDonald B, Cortina-Borja M, Herron BM, Crow TJ. The size and fibre composition of the corpus callosum with respect to gender and schizophrenia: a postmortem study. Brain 1999;122:99–110. [PubMed: 10050898]

Highley JR, Walker MA, Esiri MM, Crow TJ, Harrison PJ. Asymmetry of the uncinate fasciculus: a postmortem study of normal subjects and patients with schizophrenia. Cereb Cortex 2002;12:1218–1224. [PubMed: 12379610]

Huang H, Zhang J, Jiang H, Wakana S, Poetscher L, Miller MI, van Zijl PCM, Hillis AE, Wytik R, Mori S. DTI tractography based parcellation of white matter: application of the mid-sagittal morphology of corpus callosum. NeuroImage 2005;26:295–305.

Jernigan TL, Fennema-Notestine C. White matter mapping is needed. Neurobiol Aging 2004;25:37–39. [PubMed: 14675728]

Jiang H, van Zijl PC, Kim J, Pearlson GD, Mori S. DtiStudio: resource program for diffusion tensor computation and fiber bundle tracking. Comput Methods Programs Biomed 2006;81:106–116. [PubMed: 16413083]

Johansen-Berg, H.; Behrens, TEJ. Diffusion MRI: from quantitative measurements to in vivo neuroanatomy. Academic Press; London: 2009.

Jones DK, Catani M, Pierpaoli C, Reeves SJ, Shergill SS, O'Sullivan M, Golesworthy P, McGuire P, Horsfield MA, Simmons A, Williams SC, Howard RJ. Age effects on diffusion tensor magnetic

resonance imaging tractography measures of frontal cortex connections in schizophrenia. Hum Brain Map 2006;27:230–238.

Kubicki M, Westin CF, Maier SE, Frumin M, Nestor PG, Salisbury DF, Kikinis R, Jolesz FA, McCarley RW, Shenton ME. Uncinate fasciculus findings in schizophrenia: a magnetic resonance diffusion tensor imaging study. Am J Psychiatry 2002;159:813–820. [PubMed: 11986136]

LaMantia AS, Rakic P. Axon overproduction and elimination in the corpus callosum of the developing rhesus monkey. J Neurosci 1990;10:2156–2175. [PubMed: 2376772]

Le Bihan, D. Diffusion and perfusion magnetic resonance imaging: applications to functional MRI. Raven Press; New York: 1995.

Le Bihan D. Looking into the functional architecture of the brain with diffusion MRI. Nat Rev Neurosci 2003;4:469–480. [PubMed: 12778119]

Lebel C, Walker L, Leemans A, Phillips L, Beaulieu C. Microstructural maturation of the human brain from childhood to adulthood. Neuroimage 2008;40:1044–1055. [PubMed: 18295509]

Lenroot RK, Giedd JN. Brain development in children and adolescents: insights from anatomical magnetic resonance imaging. Neurosci Biobehav Rev 2006;30:718–729. Review. [PubMed: 16887188]

Luders E, Narr KL, Thompson PM, Rex DE, Jancke L, Toga AW. Hemispheric asymmetries in cortical thickness. Cereb Cortex 2006;16:1232–1238. [PubMed: 16267139]

Makris N, Pandya DN. The extreme capsule in humans and rethinking of the language circuitry. Brain Struct Funct 2009;213:343–358. [PubMed: 19104833]

Makris N, Worth AJ, Sorensen AG, Papadimitriou GM, Wu O, Reese TG, Wedeen VJ, Davis TL, Stakes JW, Caviness VS, Kaplan E, Rosen BR, Pandya DN, Kennedy DN. Morphometry of in vivo human white matter association pathways with diffusion-weighted magnetic resonance imaging. Ann Neurol 1997;42:951–962. [PubMed: 9403488]

Masliah E, Mallory M, Hansen L, DeTeresa R, Terry RD. Quantitative synaptic alterations in the human neocortex during normal aging. Neurology 1993;43:192–197. [PubMed: 8423884]

McLaughlin NC, Paul RH, Grieve SM, Williams LM, Laidlaw D, Dicarlo M, Clark CR, Whelihan W, Cohen RA, Whitford TJ, Gordon E. Diffusion tensor imaging of the corpus callosum: a cross-sectional study across the lifespan. Int J Dev Neurosci 2007;25:215–221. [PubMed: 17524591]

Mori, S. Introduction to Diffusion Tensor Imaging. Elsiever; Amsterdam: 2007.

Mori S, Kaufmann WE, Davatzikos C, Stieltjes B, Amodei L, Fredericksen K, Pearlson GD, Melhem ER, Solaiyappan M, Raymond GV, Moser HW, van Zijl PC. Imaging cortical association tracts in the human brain using diffusion-tensor-based axonal tracking. Magn Reson Med 2002;47:215–223. [PubMed: 11810663]

Mukherjee P, McKinstry RC. Diffusion tensor imaging and tractography of human brain development. Neuroimag Clin N Am 2006;16:19–43.

Mukherjee P, Miller JH, Shimony JS, Philip JV, Nehra D, Snyder AZ, Conturo TE, Neil JJ, McKinstry RC. Diffusion-tensor MR imaging of gray and white matter development during normal human brain maturation. AJNR Am J Neuroradiol 2002;23:1445–1456. [PubMed: 12372731]

Netsch T, van Muiswinkel A. Quantitative evaluation of image-based distortion correction in diffusion tensor imaging. IEEE Trans Med Imaging 2004;23:789–798. [PubMed: 15250631]

Nucifora PG, Verma R, Melhem ER, Gur RE, Gur RC. Leftward asymmetry in relative fiber density of the arcuate fasciculus. Neuroreport 2005;16:791–794. [PubMed: 15891571]

Ota M, Obata T, Akine Y, Ito H, Ikehira H, Asada T, Suhara T. Age-related degeneration of corpus callosum measured with diffusion tensor imaging. Neuroimage 2006;31:1445–1452. [PubMed: 16563802]

Pakkenberg B, Gundersen HJ. Neocortical neuron number in humans: effect of sex and age. J Comp Neurol 1997;384:312–320. [PubMed: 9215725]

Park HJ, Westin CF, Kubicki M, Maier SE, Niznikiewicz M, Baer A, Frumin M, Kikinis R, Jolesz FA, McCarley RW, Shenton ME. White matter hemisphere asymmetries in healthy subjects and in schizophrenia: a diffusion tensor MRI study. NeuroImage 2004;23:213–223. [PubMed: 15325368]

Partridge SC, Mukherjee P, Henry RG, Miller SP, Berman JI, Jin H, Lu Y, Glenn OA, Ferriero DM, Barkovich AJ, Vigneron DB. Diffusion tensor imaging: serial quantitation of white matter tract maturity in premature newborns. NeuroImage 2004;22:1302–1314. [PubMed: 15219602]

Paus T, Zijdenbos A, Worsley K, Collins DL, Blumenthal J, Giedd JN, Rapoport JL, Evans AC. Structural maturation of neural pathways in children and adolescents: in vivo study. Science 1999;283:1908–1911. [PubMed: 10082463]

Peled S, Gudbjartsson H, Westin CF, Kikinis R, Jolesz FA. Magnetic resonance imaging shows orientation and asymmetry of white matter fiber tracts. Brain Res 1998;780:27–33. [PubMed: 9473573]

Peters A, Sethares C. Is there remyelination during aging of the primate central nervous system? J Comp Neurol 2003;460:238–254. [PubMed: 12687688]

Pierpaoli C, Jezzard P, Basser PJ, Barnett A, Di Chiro G. Diffusion tensor MR imaging of the human brain. Radiology 1996;201:637–648. [PubMed: 8939209]

Powell HW, Parker GJ, Alexander DC, Symms MR, Boulby PA, Wheeler-Kingshott CA, Barker GJ, Noppeney U, Koepp MJ, Duncan JS. Hemispheric asymmetries in language-related pathways: a combined functional MRI and tractography study. NeuroImage 2006;32:388–399. [PubMed: 16632380]

Pujol J, Vendrell P, Junque C, Marti-Vilalta JL, Capdevila A. When does human brain development end? Evidence of corpus callosum growth up to adulthood. Ann Neurol 1993;34:71–75. [PubMed: 8517683]

Rodrigo S, Oppenheim C, Chassoux F, Golestani N, Cointepas Y, Poupon C, Semah F, Mangin JF, Le Bihan D, Meder JF. Uncinate fasciculus fiber tracking in mesial temporal lobe epilepsy. Initial findings. Eur Radiol 2007;17:1663–1668. [PubMed: 17219141]

Salat DH, Tuch DS, Greve DN, van der Kouwe AJ, Hevelone ND, Zaleta AK, Rosen BR, Fischl B, Corkin S, Rosas HD, Dale AM. Age-related alterations in white matter microstructure measured by diffusion tensor imaging. Neurobiol Aging 2005;26:1215–1227. [PubMed: 15917106]

Schwartz ED, Cooper ET, Fan Y, Jawad AF, Chin CL, Nissanov J, Hackney DB. MRI diffusion coefficients in spinal cord correlate with axon morphometry. Neuroreport 2005;16:73–76. [PubMed: 15618894]

Shin YW, Kim DJ, Ha TH, Park HJ, Moon WJ, Chung EC, Lee JM, Kim IY, Kim SI, Kwon JS. Sex differences in the human corpus callosum: diffusion tensor imaging study. Neuroreport 2005;16:795–798. [PubMed: 15891572]

Snook L, Paulson LA, Roy D, Phillips L, Beaulieu C. Diffusion tensor imaging of neurodevelopment in children and young adults. NeuroImage 2005;26:1164–1173. [PubMed: 15961051]

Song SK, Yoshino J, Le TQ, Lin SJ, Sun SW, Cross AH, Armstrong RC. Demyelination increases radial diffusivity in corpus callosum of mouse brain. NeuroImage 2005;26:132–140. [PubMed: 15862213]

Sowell ER, Peterson BS, Thompson PM, Welcome SE, Henkenius AL, Toga AW. Mapping cortical change across the human life span. Nat Neurosci 2003;6:309–315. [PubMed: 12548289]

Stadlbauer A, Salomonowitz E, Strunk G, Hammen T, Ganslandt O. Age-related degradation in the central nervous system: assessment with diffusion-tensor imaging and quantitative fiber tracking. Radiology 2008;247:179–188. [PubMed: 18292477]

Sullivan EV, Adalsteinsson E, Pfefferbaum A. Selective age related degradation of anterior callosal fiber bundles quantified in vivo with fiber tracking. Cereb Cortex 2006;16:1030–1039. [PubMed: 16207932]

Sullivan EV, Rohlfing T, Pfefferbaum A. Quantitative fiber tracking of lateral and interhemispheric white matter systems in normal aging: Relations to timed performance. Neurobiol Aging. 200910.1016/j.neurobiolaging.2008.04.007

Szeszko PR, Vogel J, Ashtari M, Malhotra AK, Bates J, Kane JM, Bilder RM, Frevert T, Lim K. Sex differences in frontal lobe white matter microstructure: a DTI study. Neuroreport 2003;14:2469–2473. [PubMed: 14663212]

Taoka T, Iwasaki S, Sakamoto M, Nakagawa H, Fukusumi A, Myochin K, Hirohashi S, Hoshida T, Kichikawa K. Diffusion anisotropy and diffusivity of white matter tracts within the temporal stem in Alzheimer disease: evaluation of the “tract of interest” by diffusion tensor tractography. AJNR Am J Neuroradiol 2006;27:1040–1045. [PubMed: 16687540]

Terao S, Sobue G, Hashizume Y, Shimada N, Mitsuma T. Age-related changes of the myelinated fibers in the human cortico-spinal tract: a quantitative analysis. Acta Neuropathol (Berl) 1994;88:137–142. [PubMed: 7985494]

Vernooij MW, Smits M, Wielopolski PA, Houston GC, Krestin GP, van der Lugt A. Fiber density asymmetry of the arcuate fasciculus in relation to functional hemispheric language lateralization in both right- and left-handed healthy subjects: a combined fMRI and DTI study. NeuroImage 2007;35:1064–1076. [PubMed: 17320414]

Wakana S, Jiang H, Nagae-Poetscher LM, van Zijl PC, Mori S. Fiber tract-based atlas of human white matter anatomy. Radiology 2004;230:77–87. [PubMed: 14645885]

Walhovd KB, Fjell AM, Reinvang I, Lundervold A, Dale AM, Eilertsen DE, Quinn BT, Salat D, Makris N, Fischl B. Effects of age on volumes of cortex, white matter and subcortical structures. Neurobiol Aging 2005;26:1261–1270. [PubMed: 16005549]

Westerhausen R, Kreuder F, Dos Santos Sequeira S, Walter C, Woerner W, Wittling RA, Schweiger E, Wittling W. Effects of handedness and gender on macro- and microstructure of the corpus callosum and its subregions: a combined high-resolution and diffusion-tensor MRI study. Brain Res Cogn Brain Res 2004;21:418–426. [PubMed: 15511657]

Westerhausen R, Huster RJ, Kreuder F, Wittling W, Schweiger E. Corticospinal tract asymmetries at the level of the internal capsule: is there an association with handedness? Neuroimage 2007;37:379–386. [PubMed: 17601751]

Xu D, Mori S, Solaiyappan M, van Zijl PC, Davatzikos C. A framework for callosal fiber distribution analysis. NeuroImage 2002;17:1131–1143. [PubMed: 12414255]

Yakovlev, PI.; LeCours, AR. The myelogenetic cycles of regional maturation of the brain. In: Minkowsky, K., editor. Regional development of the brain in early life. Blackwell; Oxford: 1967. p. 3-70.

Zahr NM, Rohlfing T, Pfefferbaum A, Sullivan EV. Problem solving, working memory, and motor correlates of association and commissural fiber bundles in normal aging: a quantitative fiber tracking study. Neuroimage 2009;44:1050–1062. [PubMed: 18977450]

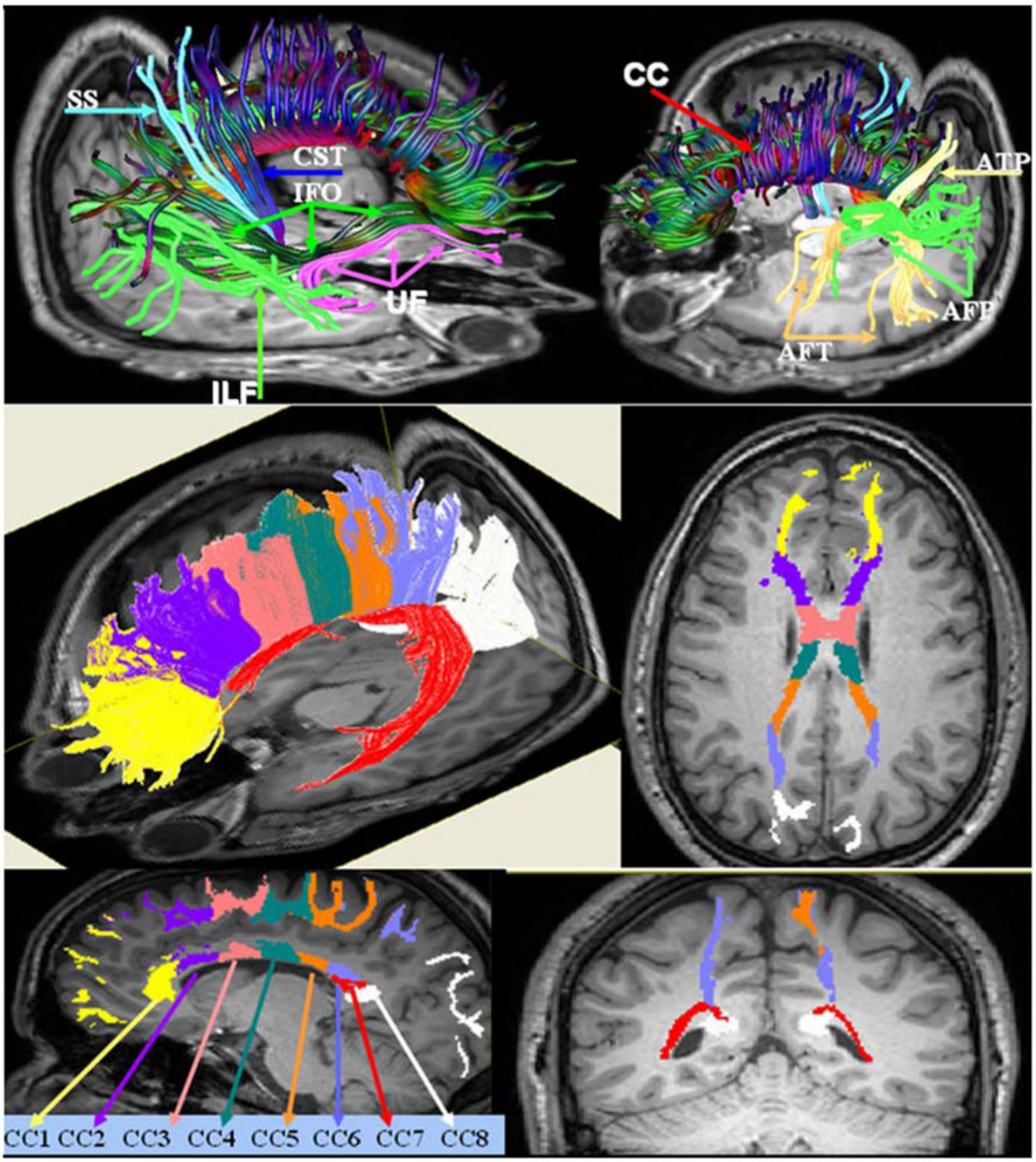

Fig. 1.
Illustration of the association, projection (*upper panel*) and commissural pathways (*lower panel*) quantified in this study

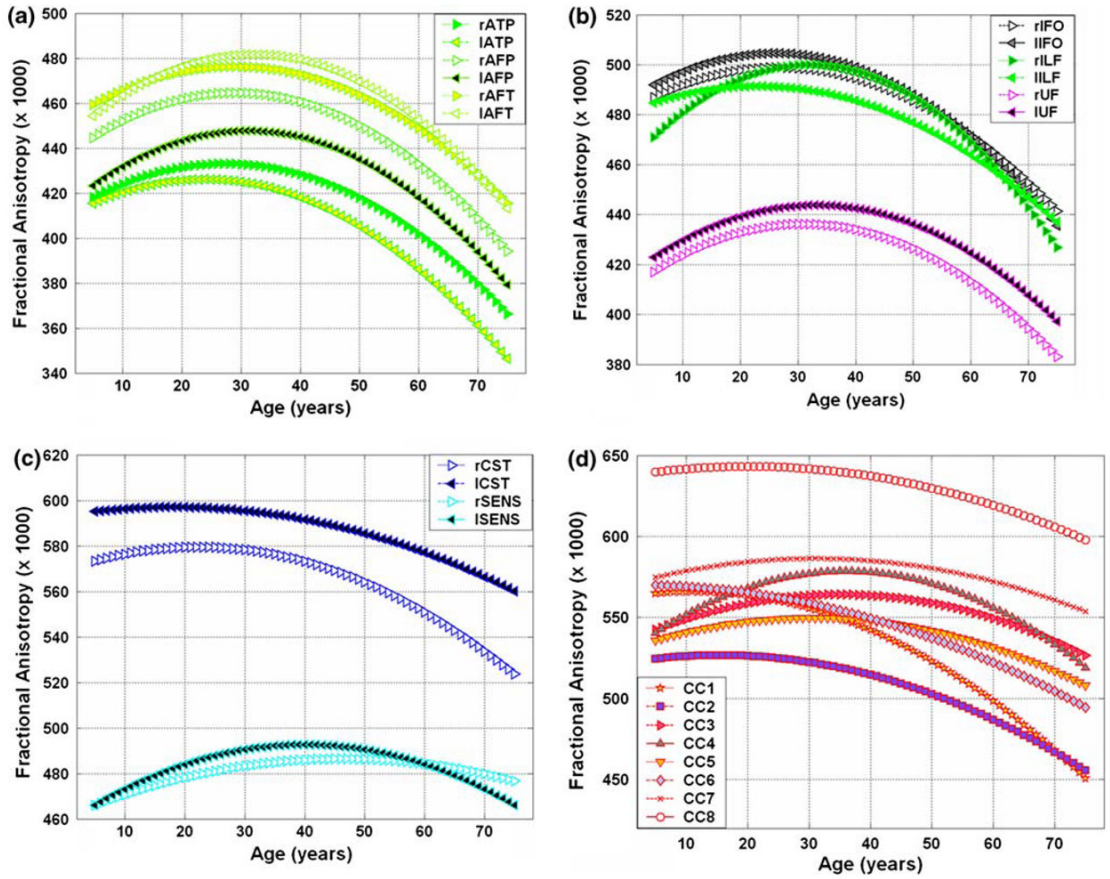

Fig. 2.

A plot of least-squares fit of the fractional anisotropy versus age of the 24 fiber tracts studied (see Table 1 for the corresponding fit parameters). **a** Arcuate fasciculus; **b** ILF, IFOF, and UF; **c** CST and SS; and **d** CC

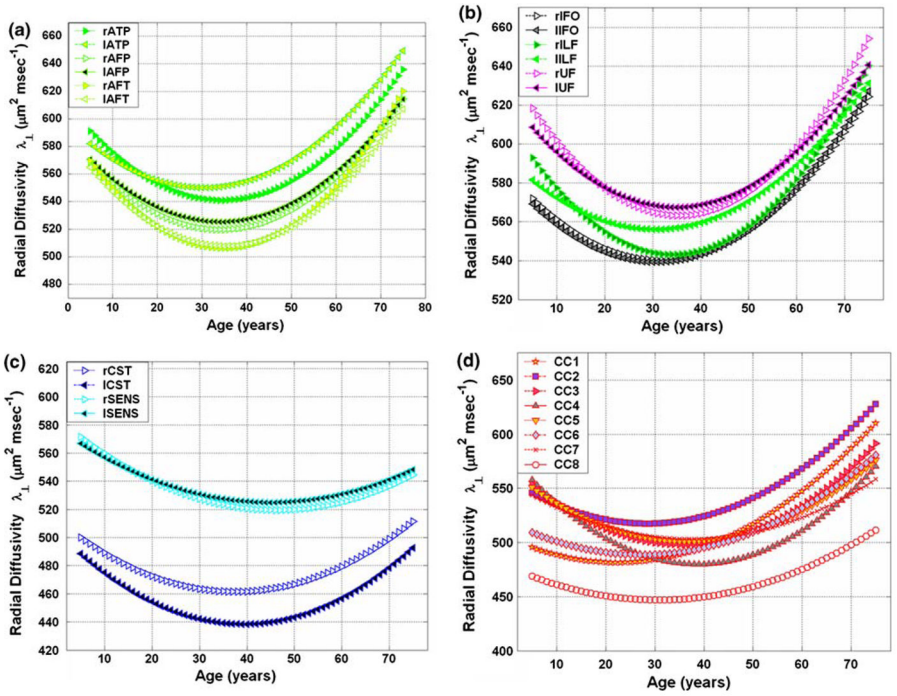

Fig. 3.

A plot of least-squares fit of the radial diffusivity versus age of the 24 fiber tracts studied (see Table 2 for the corresponding fit parameter; the axial diffusivities are provided in the Supplementary Results). **a** Arcuate fasciculus; **b** ILF, IFOF and UF; **c** CST and SS; and **d** CC

Table 1

Summary of the fractional anisotropy versus age in years least-squares fitted results on the 24 fiber tracts along with the standard errors and significant *p* values

Fiber tracts fractional anisotropy		$y = \beta_0 + \beta_1 \times age + \beta_2 \times age^2$		
		$\beta_0 \pm SD$	$\beta_1 \pm SD$	$\beta_2 \pm SD$
Association pathways				
ATP	R	410.74 ± 9.35*	1.62 ± 0.63†	−0.030 ± 0.009†
93 (24C, 69A)	L	408.86 ± 10.93*	1.45 ± 0.73‡	−0.030 ± 0.011†
AFP	R	435.46 ± 7.68*	1.99 ± 0.51*	−0.034 ± 0.007*
98 (25C, 73A)	L	413.098 ± 9.214*	2.22 ± 0.61*	−0.036 ± 0.009*
AFT	R	451.76 ± 10.42*	1.68 ± 0.67†	−0.029 ± 0.009†
69 (16C, 53A)	L	443.41 ± 10.39*	2.39 ± 0.67†	−0.037 ± 0.009*
IFOF	R	480.79 ± 9.25*	1.35 ± 0.62†	−0.025 ± 0.009†
104 (28C, 76A)	L	485.20 ± 10.39*	1.50 ± 0.61†	−0.029 ± 0.009*
ILF	R	459.21 ± 8.25*	2.54 ± 0.56*	−0.040 ± 0.008*
103 (29C, 74A)	L	480.58 ± 7.75*	0.93 ± 0.53‡	−0.020 ± 0.008†
UF	R	408.87 ± 9.52*	1.75 ± 0.65†	−0.028 ± 0.009†
100 (29C, 71A)	L	414.76 ± 8.66*	1.75 ± 0.60†	−0.026 ± 0.009†
Projection pathways				
CST	R	569.22 ± 10.81*	0.92 ± 0.76‡	−0.020 ± 0.011‡
93 (27C, 66A)	L	593.35 ± 10.07*	0.41 ± 0.71‡	−0.011 ± 0.011‡
Sensory	R	460.72 ± 10.54*	1.11 ± 0.71‡	−0.012 ± 0.010‡
92 (25C, 67A)	L	457.93 ± 10.58*	1.74 ± 0.71†	−0.022 ± 0.010†
Commissural (corpus callosum) pathways				
CC1 (prefrontal)		562.56 ± 8.90*	0.613 ± 0.623‡	−0.028 ± 0.009†
CC2 (anterior frontal)		521.89 ± 8.56*	0.62 ± 0.60‡	−0.020 ± 0.009†
CC3 (superior frontal)		534.54 ± 8.47*	1.68 ± 0.59†	−0.024 ± 0.009†
CC4 (posterior frontal)		527.15 ± 10.69*	2.85 ± 0.75*	−0.039 ± 0.011*
CC5 (anterior parietal)		529.78 ± 10.43*	1.30 ± 0.73‡	−0.021 ± 0.011*
CC6 (posterior parietal)		570.02 ± 10.31*	0.05 ± 0.72‡	−0.014 ± 0.011‡
CC7 (temporal)		569.94 ± 10.47*	−0.02 ± 0.01‡	−0.017 ± 0.011‡
CC8 (occipital)		637.08 ± 8.51*	0.61 ± 0.60‡	−0.015 ± 0.009‡

Age at peak (in years) and standard deviation (SD) were computed assuming significant fit model (linear and quadratic) coefficients as detailed in the "Methods"

NA not available as any of the linear or quadratic terms was not significant

* $p < 0.0001$

† $p < 0.05$

$^{\ddagger}p = 0.08$

Table 2

Summary of the radial diffusivity versus age in years least-squares fitted results on the 24 fiber tracts along with the standard errors and significant *p* values

Fiber tracts radial diffusivity		Fit model: $y = \beta_0 + \beta_1 \times \text{age} + \beta_2 \times \text{age}^2$			Age at peak
		$\beta_0 \pm$ SD	$\beta_1 \pm$ SD	$\beta_2 \pm$ SD	
Association pathways					
ATP 93 (24C, 69A)	R	609.7 ± 11.4*	−3.99 ± 0.76*	0.058 ± 0.011*	34.5 ± 9.3
	L	596.1 ± 12.4*	−3.02 ± 0.83*	0.050 ± 0.012*	30.4 ± 11.1
AFP 98 (25C, 73A)	R	586.6 ± 11.1*	−3.92 ± 0.73*	0.057 ± 0.010*	34.2 ± 8.8
	L	587.6 ± 12.3*	−3.65 ± 0.81*	0.053 ± 0.011*	34.2 ± 10.5
AFT 69 (16C, 53A)	R	592.5 ± 13.5*	−4.94 ± 0.86*	0.071 ± 0.012*	34.9 ± 8.4
	L	585.4 ± 13.1*	−4.41 ± 0.83*	0.063 ± 0.011*	35.2 ± 9.3
IFOF 104 (28C, 76A)	R	585.0 ± 10.0*	−2.82 ± 0.67*	0.045 ± 0.010*	31.6 ± 10.2
	L	581.9 ± 9.8*	−2.77 ± 0.66*	0.045 ± 0.009*	30.8 ± 9.8
ILF 103 (29C, 74A)	R	611.4 ± 10.3*	−3.99 ± 0.70*	0.058 ± 0.010*	34.2 ± 8.4
	L	592.3 ± 10.0*	−2.36 ± 0.68†	0.038 ± 0.010*	30.7 ± 11.8
UF 100 (29C, 71A)	R	637.8 ± 11.8*	−4.19 ± 0.81*	0.059 ± 0.012*	35.6 ± 9.9
	L	623.4 ± 11.4*	−3.20 ± 0.78*	0.046 ± 0.011*	35.0 ± 12.1
Projection pathways					
CST 93 (27C, 66A)	R	512.9 ± 10.9*	−2.73 ± 0.76†	0.036 ± 0.011†	37.7 ± 15.9
	L	504.4 ± 11.6*	−3.35 ± 0.81*	0.043 ± 0.012†	39.3 ± 14.7
Sensory 92 (25C, 67A)	R	584.8 ± 15.6*	−2.82 ± 1.05†	0.030 ± 0.015†	46.3 ± 28.6
	L	578.0 ± 15.4*	−2.36 ± 1.04†	0.026 ± 0.015‡	~45 ± 32
Commissural pathways: 31 children (14B, 17G) and 68 adults (25 M, 43 W)					
CC1 (prefrontal)		504.7 ± 10.8*	−2.08 ± 0.75†	0.046 ± 0.011*	22.4 ± 9.7
CC2 (anterior frontal)		559.1 ± 10.4*	−2.92 ± 0.73*	0.051 ± 0.011*	28.6 ± 9.3
CC3 (superior frontal)		573.3 ± 11.1*	−4.23 ± 0.77*	0.060 ± 0.011*	35.5 ± 9.4
CC4 (posterior frontal)		582.4 ± 14.1*	−5.30 ± 0.99*	0.068 ± 0.015*	38.7 ± 11.0
CC5 (anterior parietal)		567.8 ± 13.2*	−3.66 ± 0.92*	0.050 ± 0.014*	36.4 ± 13.5

Fiber tracts radial diffusivity	Fit model: $y = \beta_0 + \beta_1 \times \text{age} + \beta_2 \times \text{age}^2$			Age at peak
	$\beta_0 \pm$ SD	$\beta_1 \pm$ SD	$\beta_2 \pm$ SD	
CC6 (posterior parietal)	$519.1 \pm 13.5^{*}$	$-2.22 \pm 0.95^{*}$	$0.041 \pm 0.014^{\dagger}$	27.4 ± 15.0
CC7 (temporal)	$557.6 \pm 13.8^{*}$	$-2.92 \pm 0.96^{*}$	$0.039 \pm 0.014^{\dagger}$	37.3 ± 18.3
CC8 (occipital)	$478.1 \pm 12.5^{*}$	$-2.03 \pm 0.88^{\dagger}$	$0.033 \pm 0.013^{\dagger}$	30.7 ± 18.0

Age at peak (in years) and standard deviation (SD) were computed assuming significant fit model (linear and quadratic) coefficients as detailed in the “Methods”

NA not available as any of the linear or quadratic terms was not significant

$^{*}p < 0.0001$

$^{\dagger}p < 0.05$

$^{\ddagger}p = 0.08$